Volume Title
*ASP Conference Series, Vol. **Volume Number***
Author

Momentum-driven feedback and the M-σ relation in non-isothermal galaxies

Rachael C. McQuillin and Dean E. McLaughlin

Astrophysics Group, Lennard Jones Laboratories, Keele University, Keele, Staffordshire, ST5 5BG, UK

Abstract. We solve for the velocity fields of momentum-conserving supershells driven by feedback from supermassive black holes or nuclear star clusters (central massive objects: CMOs). We treat, for the first time, the case of CMOs embedded in gaseous protogalaxies with non-isothermal dark matter haloes having peaked circular-speed profiles. We find the CMO mass that is sufficient to drive *any* shell to escape *any* such halo. In the limit of large halo mass, relevant to real galaxies, this critical CMO mass depends only on the peak circular speed in the halo, scaling as $M_{\rm crit} \propto V^4_{\rm c,pk}$.

1. Introduction

The M–σ relation between supermassive black hole (SMBH) mass (e.g., Gültekin et al. 2009) or nuclear star cluster (NC) mass (Ferrarese et al. 2006) and the stellar velocity dispersion of galaxy bulges can be understood as a result of momentum-conserving feedback (e.g., King 2005; McLaughlin et al. 2006). Recently, Volonteri et al. (2011) have argued that SMBH mass also correlates with the asymptotic circular speed at large radii in bulges. Such an M–$V_{\rm c}$ relation should presumably also be related to feedback, a point that we investigate in McQuillin & McLaughlin (2012) and summarize here.

Accretion at near- or super-Eddington rates onto an SMBH in a gaseous protogalaxy is expected to result in a fast wind driven back into the galaxy. Similarly, the winds and supernovae from massive stars in a young NC will drive a superwind into its host galaxy. In a spherical approximation to either case, the wind from the central massive object (CMO) sweeps ambient gas into a shell that, at least initially, cools rapidly and is therefore momentum-driven (King 2003; McLaughlin et al. 2006). For a CMO larger than some critical mass, the wind thrust ($\propto M_{\rm CMO}$) can overcome the gravity of the host dark matter halo (measured by σ) and the shell can escape, cutting off fuel to the CMO and locking in an $M_{\rm CMO}$–σ relation and associated scalings.

King (2005) showed that the CMO mass required to drive a shell at large radius in a singular isothermal sphere with velocity dispersion σ_0 is

$$M_\sigma \;\equiv\; f_0 \kappa \sigma_0^4 / (\pi G^2 \lambda) \;=\; 4.56\times 10^8 \; M_\odot \, \sigma_{200}^4 \, f_{0.2} \, \lambda^{-1} \;\; , \qquad (1)$$

where f_0 is a gas mass fraction (assumed to be spatially constant, and with $f_0 \approx 0.2$ so $f_{0.2} = f_0/0.2$); κ is the electron scattering opacity; and $\sigma_{200} = \sigma_0/200\,{\rm km\,s^{-1}}$. The parameter λ is related to the feedback efficiency of each CMO type: $\lambda \approx 1$ for SMBHs, and $\lambda \approx 0.05$ for NCs (McLaughlin et al. 2006). In McQuillin & McLaughlin (2012), we derive a version of eq. (1) for *non-isothermal* dark matter haloes. In this more realistic and general case, the critical CMO mass depends on a *peak circular speed*.

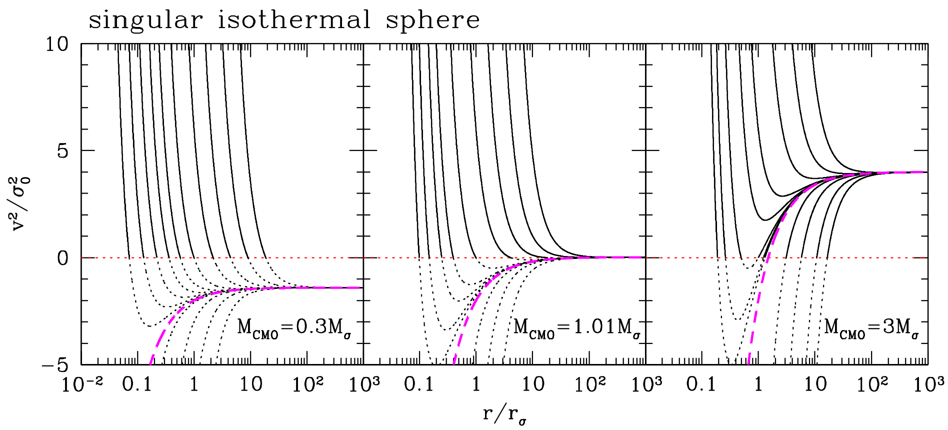

Figure 1. Velocity fields, v^2 versus r, for momentum-driven shells in a singular isothermal sphere with spatially constant gas fraction (eq. [4]). The long-dashed curve in each panel is the solution with $C = 0$ for the CMO mass indicated. The physical ($v^2 \geq 0$) parts of solutions with $C \neq 0$ are shown as solid lines. The mass unit M_σ is defined in eq. (1); the radius unit is $r_\sigma \equiv GM_\sigma/\sigma_0^2 \simeq 49$ pc σ_{200}^2.

2. Velocity Fields of Momentum-Driven Shells

We assume that the CMO wind thrust is $dp_{\rm wind}/dt = \lambda L_{\rm Edd}/c$ (King & Pounds 2003; McLaughlin et al. 2006). The equation of motion for a momentum-driven shell in any dark matter halo profile $M_{\rm DM}(r)$ is therefore (see also King 2005)

$$\frac{d}{dt}\left[M_{\rm g}(r)v\right] = \frac{4\pi G\lambda M_{\rm CMO}}{\kappa} - \frac{GM_{\rm g}(r)}{r^2}\left[M_{\rm CMO} + M_{\rm DM}(r)\right] \quad . \tag{2}$$

Here r is the instantaneous radius of the shell; $v = dr/dt$ is the velocity of the shell; and $M_{\rm g}(r)$ is the ambient gas mass originally inside radius r (i.e., the mass that has been swept up into the shell when it has radius r). Then, letting $M_{\rm g}(r) \equiv f_0\, h(r)\, M_{\rm DM}(r)$, where $h(r)$ is a function describing how the gas traces the dark matter [i.e., $h(r) \equiv 1$ when the gas traces the dark matter directly], we re-write eq. (2) to solve for the velocity field $v(r)$ rather than $r(t)$ directly:

$$\frac{d}{dr}\left[M_{\rm DM}^2 h^2 v^2(r)\right] = \frac{8\pi G\lambda}{f_0\kappa} M_{\rm CMO} h(r) M_{\rm DM}(r) - \frac{2M_{\rm DM}^2(r)h^2(r)}{r^2}\left[M_{\rm CMO} + M_{\rm DM}(r)\right] \quad . \tag{3}$$

3. Singular Isothermal Sphere

We first revisit the singular isothermal sphere, in which $M_{\rm DM}(r) = 2\sigma_0^2 r/G$. With this mass profile and $h(r) \equiv 1$, so the gas traces the dark matter directly, eq. (3) has solution

$$v^2 = 2\sigma_0^2\left[\frac{M_{\rm CMO}}{M_\sigma} - 1\right] - \frac{2GM_{\rm CMO}}{r} + \frac{C}{r^2} \quad , \tag{4}$$

where M_σ is defined in eq. (1) and the constant of integration, C, represents the shell momentum at $r = 0$. This solution is only physical if $v^2 > 0$. At arbitrarily large

radius, the shell tends to a constant coasting speed, $v_\infty^2 \equiv 2\sigma_0^2\,[M_{\rm CMO}/M_\sigma - 1]$, so that $M_{\rm CMO} > M_\sigma$ is required for shells to move at all at large r. This is fundamentally the result of King (2005). But at small radius, the term C/r^2 in eq. (4) dominates and the behaviour of a shell is determined by its initial momentum.

Figure 1 plots v^2 versus r from eq. (4) for $M_{\rm CMO}/M_\sigma$ =0.3, 1.01 and 3, with a range of C values in each case. When $M_{\rm CMO} < M_\sigma$ (left panel), no shell can ever escape. All solutions either have the shell stalling (i.e., crossing $v^2 = 0$) at a finite radius, or are unphysical ($v^2 < 0$) at all radii. When $M_{\rm CMO} = 1.01 M_\sigma$ (middle panel), only a few solutions formally allow shells to reach large r without stalling. However, these potential escapes require initial ($r = 0$) shell momenta, C, so large as to give velocities $v \gtrsim 0.2\,c\,\sigma_{200}$ at radii $r \sim 1$ pc σ_{200}^2; and even then, they tend to a large-r coasting speed of just $v_\infty = 0.14\,\sigma_0$. Thus, $M_{\rm CMO} > M_\sigma$ is a *necessary but not sufficient* condition for the escape of momentum-driven feedback from an isothermal sphere. For $M_{\rm CMO} = 3M_\sigma$ (right panel), the ability to reach large radii still depends on the initial momentum of the shell. Shells decelerating from small radius require $v \gtrsim 0.05\,c\,\sigma_{200}$ at $r \sim 1$ pc σ_{200}^2 to avoid stalling. Launch solutions (those accelerating outwards from $v^2 = 0$ at a non-zero radius) are also possible, but only starting from radii $r \gtrsim 40$ pc σ_{200}^2.

In the case $M_{\rm CMO} = 3M_\sigma$, the shells that reach large radii eventually coast at $v_\infty = 2\sigma_0$, which is the escape speed from an isothermal sphere. We conclude that at least $M_{\rm CMO} \geq 3M_\sigma$ is required (along with a large shell momentum at $r = 0$) for escape. The objection by Silk & Nusser (2010) to momentum-conserving black hole winds as the sole source of the SMBH M–σ relation ultimately traces back to our result for v_∞^2. However, *the problem is specific to the assumption of an isothermal dark matter halo*.

4. Non-Isothermal Dark Matter Haloes

More realistically, dark matter haloes have density profiles that are shallower than isothermal at small radii and steeper than isothermal at large radii. The circular speed, $V_{\rm c}^2 = GM_{\rm DM}(r)/r$, corresponding to any such density profile increases outwards from the centre, has a well-defined peak, and then declines towards larger radii. As a result, momentum-driven shells always accelerate at large radii (McQuillin & McLaughlin 2012) and are guaranteed to exceed the halo escape speed eventually, just so long as they do not stall before reaching radii where they can begin to accelerate.

The natural velocity unit in such non-isothermal haloes is the peak value of the circular speed, $V_{\rm c,pk}$, and we define the associated mass

$$M_\sigma \equiv \frac{f_0 \kappa}{\lambda \pi G^2}\,\frac{V_{\rm c,pk}^4}{4} = 1.14 \times 10^8\ M_\odot \left(\frac{V_{\rm c,pk}}{200\,{\rm km\,s^{-1}}}\right)^4 f_{0.2}\,\lambda^{-1} \ . \qquad (5)$$

An obvious choice of fiducial velocity dispersion here is $\sigma_0 \equiv V_{\rm c,pk}/\sqrt{2}$, for which eq. (5) reduces to eq. (1). In either form, given our results for the isothermal sphere above and for other halo models below (e.g., Figure 3), M_σ is best viewed as just a unit.

A general analysis of equation (3) shows that, in any dark matter halo with a single-peaked circular-speed curve, there is a critical CMO mass, $M_{\rm crit}$, that *is sufficient* to guarantee the escape of shells with *any initial momentum* (McQuillin & McLaughlin 2012). This $M_{\rm crit}$ depends primarily on $V_{\rm c,pk}$ and on the dark matter mass, $M_{\rm pk}$, within the peak of the circular-speed curve. In the limit that $M_{\rm pk} \gg M_\sigma$, which is most

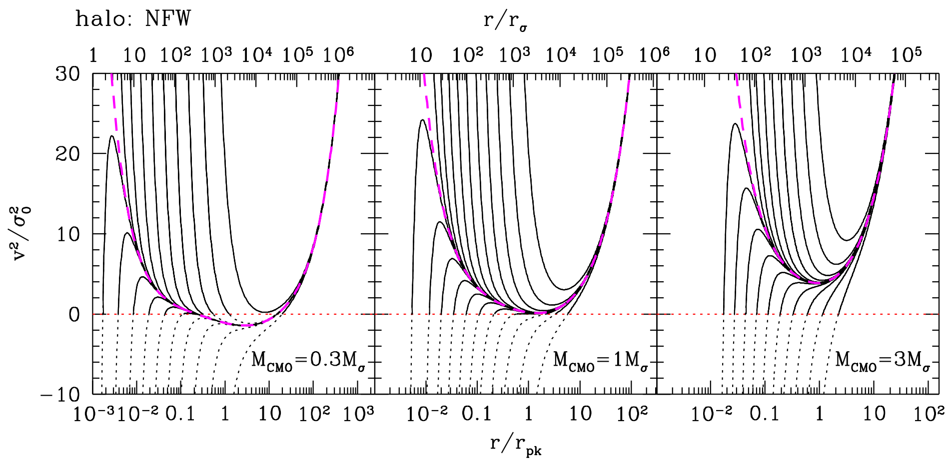

Figure 2. Velocity fields for momentum-driven shells in a Milky Way-sized, NFW halo with spatially constant gas fraction. Long-dashed curves represent solutions with zero momentum at $r = 0$. Velocities are put in units of $\sigma_0 \equiv V_{\rm c,pk}/\sqrt{2}$. The mass unit M_σ is defined in eq. (5). The radius unit on the lower axis is the radius at which the dark matter circular-speed curve peaks; in the Milky Way, $r_{\rm pk} \approx 50$ kpc. On the upper axis, $r_\sigma \equiv GM_\sigma/(V^2_{\rm c,pk}/2) \simeq 24$ pc $(V_{\rm c,pk}/200 \text{ km s}^{-1})^2$.

relevant for real galaxies, we find that $M_{\rm crit}$ tends to a value that is independent of any other details (i.e., the exact shape) of the dark matter mass profile:

$$M_{\rm crit} \simeq M_\sigma \left[1 + M_\sigma/M_{\rm pk} + O\left(M_\sigma^2/M_{\rm pk}^2\right)\right] \longrightarrow M_\sigma \ . \qquad (M_{\rm pk} \gg M_\sigma) \qquad (6)$$

We have applied our general analysis to the specific dark matter halo models of Hernquist (1990), Navarro et al. (1997, NFW), and Dehnen & McLaughlin (2005). Figure 2, from McQuillin & McLaughlin (2012), shows numerical solutions of eq. (3) for the velocity fields of momentum-driven shells in an NFW halo with parameters appropriate to an $L_\star$ galaxy: a dark matter circular-speed curve peaking at $r_{\rm pk} = 50$ kpc with $V_{\rm c,pk} = 200$ km s^{-1}, and thus a dark matter mass of $M_{\rm pk} \simeq 4.7 \times 10^{11}\, M_\odot$ inside $r_{\rm pk}$. Equations (5) and (6) then give $M_{\rm crit} \simeq 1.00024\, M_\sigma$ for the critical CMO mass.

The left panel of Figure 2 shows v^2 versus r for shells with different initial momenta, given $M_{\rm CMO} = 0.3\, M_\sigma$. Shells that decelerate from large velocity at small radius hit $v^2 = 0$ and stall, unless they have an impossible $v \gtrsim 10^6\, c$ at $r \sim 1$ pc. Shells launched from radii $r < r_{\rm pk}$ go on to stall at some larger radius, which is still inside $r_{\rm pk}$. Launches from $r > r_{\rm pk}$ accelerate monotonically outwards and therefore always escape, but they only ever start from implausibly large $r \gtrsim 500$ kpc. By contrast, when $M_{\rm CMO} = M_\sigma$ (middle panel), all the solutions shown are able to escape, regardless of their initial velocities or momenta—as expected, since $M_{\rm crit}$ is so near M_σ here. The right-hand panel of the figure confirms that all shells escape for larger CMO masses.

The solid line in Figure 3 shows the CMO mass $M_{\rm crit}$ that is sufficient for the escape of *any* momentum-driven shell from an NFW halo, as a function of the halo mass $M_{\rm pk}$. As expected from eq. (6), $M_{\rm crit} \to M_\sigma$ for large $M_{\rm pk} \gg M_\sigma$. The dashed line in the figure shows the CMO mass that is *necessary* for the escape of shells with zero momentum at $r = 0$ *specifically*. This is slightly smaller than the sufficient CMO $M_{\rm crit}$ at any halo mass, tending to a value of $\simeq 0.94\, M_\sigma$ for $M_{\rm pk} \gg M_\sigma$.

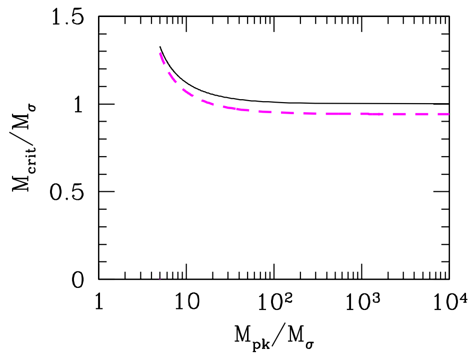

Figure 3. *Solid line*: the CMO mass (in units of M_σ defined by eq. [5]) that is *sufficient* for the escape of *any* momentum-driven shell from an NFW halo with dark matter mass $M_{\rm pk}$ inside the peak of its circular speed curve. *Dashed line*: the *necessary* CMO mass for the escape of shells with initial momentum zero *specifically*.

5. Conclusion

The critical CMO mass of King (2003, 2005; eq. [1]) is necessary but *not sufficient* for the escape of momentum-driven feedback from *isothermal* protogalaxies. By contrast, in *non-isothermal* dark matter haloes with realistic, single-peaked circular-speed curves, equations (5) and (6) above give a CMO mass that *is sufficient* for the escape of *any* momentum-driven shell: $M_{\rm crit} \simeq 1.14 \times 10^8\ M_\odot\ (V_{\rm c,pk}/200\ {\rm km\ s^{-1}})^4\ f_{0.2}\ \lambda^{-1}$, if the haloes are massive (essentially, $M_{\rm pk} \gg M_{\rm crit}$) and have spatially constant gas mass fractions. Our full analysis can be found in McQuillin & McLaughlin (2012).

Our results directly predict an $M_{\rm CMO}$–$V_{\rm c,pk}$ relation, and thus provide a basis from which to address claimed relations between SMBH mass and asymptotic circular speed in bulges (e.g., Volonteri et al. 2011). The characteristic galaxy velocity dispersion that is relevant to observed $M_{\rm CMO}$–σ relations is then $\sigma_0 \equiv V_{\rm c,pk}/\sqrt{2}$—although it is an open issue how this relates generally to measured velocity dispersions within the *stellar* effective radii of bulges. Meanwhile, working in terms of $V_{\rm c,pk}$ seems a natural way to extend the analysis of galaxy–CMO correlations to systems with significant rotational support as well as pressure support. This could be of particular interest in connection with NCs in intermediate-mass early-type galaxies, and even in bulgeless Sc/Sd disks.

References

Dehnen, W., & McLaughlin, D. E. 2005, MNRAS, 363, 1057
Gültekin et al. 2009, ApJ, 698, 198
Ferrarese et al. 2006, ApJ, 664, 17
Hernquist, L. 1990, ApJ, 356, 359
King, A. R. 2003, ApJ, 596, L27
King, A. R. 2005, ApJ, 635, L121
King A. R., & Pounds, K. A. 2003, MNRAS, 345, 657
McLaughlin, D. E., King, A. R., & Nayakshin, S. 2006, ApJ, 650, L37
McQuillin, R. C., & McLaughlin, D. E. 2012, MNRAS, submitted
Navarro, J. F., Frenk, C. S., & White, S. D. M. 1997, ApJ, 490, 493
Silk, J., & Nusser, A. 2010, ApJ, 725, 556
Volonteri, M., Natarajan, P., & Gültekin, K. 2011, ApJ, 737, 50